

## SECTION 2

### MODELING OF WIRE ROPE ISOLATORS

Wire rope isolators have different response characteristics depending on the diameter of the wire rope, the number of strands, the cable length, the cable twist, the number of cables per section and on the direction of the applied force.

To determine their dynamic characteristics in the horizontal and vertical directions, a series of dynamic tests was conducted on a number of isolators by imposing cyclic sinusoidal motion of specified amplitude, frequency and initial force. In both cases a hydraulic actuator, which was driven in displacement - controlled mode, was used to impose the motion and a load cell that was placed between the isolator and the actuator recorded the applied forces.

Five wire rope isolators were selected for testing. Their geometrical characteristics are presented in Table 2-I with reference to Figure 2-1. The first four of these isolators were later used in the isolation of an equipment cabinet in which the isolators supported its weight. During shake table testing, these isolators were subjected to simultaneous compression/tension and roll motions (see Fig. 2-1). Accordingly, component testing was restricted to only these two directions. The fifth isolator (No.5 in Table 2-I) was used in the isolation of a computer equipment which was

supported by casters. In this application, the isolators were subjected to only shearing motion (see Fig. 2-1) without allowance for vertical motion. They were, accordingly, tested only in that direction.

Wire rope isolators exhibit non-linear hysteretic behavior. In applications in which the isolators carry the weight of the isolated equipment, they are subjected to simultaneous motions in all three directions. It is, thus, expected that the forces which develop in these three directions exhibit interaction. In modeling the behavior of the isolators, it was assumed that this interaction is not important and that each isolator may be modeled by three hysteretic non-interacting spring elements placed along the three principal directions (vertical, roll and shear).

### 2.1 Testing and Modeling in Horizontal Direction.

Isolators No. 1 to 4 (Table 2-I) were tested in the roll direction by the arrangement of Figure 2-2. The arrangement could impose motion in the roll direction while allowing for some limited displacement in the vertical direction. This resembled the behavior of the isolators in actual use in which they are allowed to reduce in height during horizontal deformation. However, the arrangement could not precisely simulate the actual conditions, so that some stiffening of the isolators was observed at large horizontal displacements. This stiffening was disregarded in the modeling.

Tests were conducted by imposing five cycles of motion of frequencies of 0.1, 1, 2 and 5 Hz and amplitude of 0.25, 0.5 and 0.75 inches (6.4, 12.7 and 19.1 mm). Recorded force -displacement loops showed stable hysteretic behavior for all five cycles, symmetry and independency to frequency.

The recorded behavior represented classical hysteretic behavior and could be easily modeled by the smooth bilinear hysteretic model of Bouc, 1971. The model, in its more general form of Wen, 1976 is

$$F = \alpha \frac{F_y}{Y} U + (1 - \alpha) F_y Z \quad (2-1)$$

where  $F$  = force,  $U$  = displacement and  $Z$  is a hysteretic dimensionless quantity given by the following differential equation :

$$Y\dot{Z} + \gamma |\dot{U}| Z |Z|^{n-1} + \beta \dot{U} |Z|^n - A\dot{U} = 0 \quad (2-2)$$

In the above equations  $\alpha$ ,  $\beta$ ,  $\gamma$ ,  $A$  and  $n$  are dimensionless quantities that control the shape of the hysteretic loop, and  $F_y$  and  $Y$  are the yield force and yield displacement, respectively. A dot denotes differentiation with respect to time.

It should be noted that for  $A = 1$  and  $\beta + \gamma = 1$ , Constantinou and Adnane, 1987 have shown that the model

collapses to a model of viscoplasticity that was proposed by Ozdemir, 1976. For the analytical modeling of wire rope isolators, the values of  $\beta=0.1$ ,  $\gamma=0.9$ ,  $A=1$  and  $n=1$  were used. Appropriate values for the yield displacement,  $Y$ , were evaluated from the experimental results with  $F_y$  and  $\alpha$  calculated in each case by the following equations:

$$F_y = Q + K_x Y \quad (2-3)$$

$$\alpha = \frac{K_x Y}{F_y} \quad (2-4)$$

where  $Q$  is the characteristic strength and  $K_x$  is the stiffness in the roll direction according to the bilinear model depicted in Figure 2-3. It should be noted that  $\alpha$  represents the ratio of post-yielding to pre-yielding stiffnesses.

The parameters of the model in the roll direction of isolators No.1 to 4 are given in Table 2-II. Comparisons of experimental and analytical force - displacement loops are presented in Figures 2-4 to 2-6. It may be seen that the analytical model predicts well the experimental results.

Testing of isolator No.5 was conducted with a different arrangement which maintained constant height of the isolator during deformation in shear. Figure 2-7 shows the testing arrangement. Two isolators were connected to a plate which was driven by an actuator. Results for a single isolator were obtained by dividing the recorded force by two. The

behavior in shear of isolator No.5 was qualitatively the same as that of the other isolators in roll. The model of equations 2-1 and 2-2 reproduced well the experimental response as illustrated in Figure 2-8. The parameters of the model are given in Table 2-II.

## 2.2 Testing and Modeling in Vertical Direction.

All isolators were tested in the vertical (compression - tension) direction by the arrangement of Figure 2-9. The hysteretic behavior of the isolators in the vertical direction exhibited asymmetry due to different stiffnesses in tension and in compression. Figure 2-10 provides evidence for this behavior. The shown force - displacement loop in compression -tension is for isolator No.3. In compression, the isolator exhibits essentially elastoplastic behavior while in tension it exhibits an increasingly stiffening behavior. Figure 2-11 shows loops of the same isolator when subjected to cyclic motion at frequencies ranging from 0.1 to 5 Hz. The differences on the tension side among the various loops are due primarily to the inertia effects of the testing arrangement and the fact that the amplitude of 0.5 inch (12.7 mm) was not achieved in all cycles. It should be noted that energy dissipation, as expressed by the difference between the loading and unloading branches of the loops, is different in tension than it is in compression.

Hysteretic models for describing asymmetric behavior of the type shown in Figures 2-10 and 2-11 could be derived by a modification of the model of equations 2-1 and 2-2. The force - displacement relation is written in the form

$$F = F_0(U) + F_D(U) Z \quad (2-5)$$

in which  $F_0$  represents the displacement (U) - dependent skeleton curve and  $F_D(U)$  is the also displacement - dependent half difference between the loading and unloading branches of the loop. Z is a hysteretic dimensionless quantity taking values in the interval [-1, 1] and is described by equation 2-2. The two parts of equation 2-5 describe, respectively, stiffness and hysteretic energy dissipation.

Experimental force - displacement loops, like the one of Figure 2-10, indicated that functions  $F_0$  and  $F_D$  could be expressed in the form:

$$F_0(U) = Q_1 \cdot [A_0 - \exp(\sum_{n=1}^N a_n \cdot U^n)] \quad (2-6)$$

$$F_D(U) = Q_2 \cdot \exp[\sum_{m=0}^M b_m \cdot U^m] \quad (2-7)$$

in which  $Q_1$ ,  $A_0$ ,  $a_n$ ,  $N$ ,  $Q_2$ ,  $M$  and  $b_m$  are coefficients derived from regression analysis of experimental results for each isolator. Values of these coefficients for the tested wire rope isolators are presented in Tables 2-III and 2-IV.

For a complete description of the model of equations 2-2 and 2-5 to 2-7 it is required that parameters  $\beta$ ,  $\gamma$ ,  $A$  and  $n$  in equation 2-2 are determined. For this, an investigation of equation 2-2 is in order. Analytical solutions of this equation are possible for the ascending and, separately, for the descending branches of the  $Z - U$  loop. Concentrating on the ascending branch for which  $Z$  and  $\dot{U}$  are larger than zero, we write equation 2-2 in the form

$$\dot{Z} + (\beta + \gamma)Z^n \left( \frac{\dot{U}}{Y} \right) = A \left( \frac{\dot{U}}{Y} \right) \quad (2-8)$$

The solution is (Kamke 1959)

$$Z = \left( -\frac{A}{\beta + \gamma} \right)^{\frac{1}{n}} \cdot y(t) \quad (2-9)$$

$$\int \frac{dy}{1 + y^n} = A \left( -\frac{\beta + \gamma}{A} \right)^{\frac{1}{n}} \left( \frac{U}{Y} \right) + C \quad (2-10)$$

where  $C$  is a constant of integration. Furthermore, equation 2-8 may be written as

$$Y \frac{dZ}{dU} = A - (\beta + \gamma)Z^n \quad (2-11)$$

from where in the limit  $\frac{dZ}{dU} = 0$  the maximum value of  $Z$  is obtained

$$Z_{\max} = \left( \frac{A}{\beta + \gamma} \right)^{\frac{1}{n}} \quad (2-12)$$

The solution for the descending branch is given by equations 2-9 and 2-10 but with  $Z$  replaced by  $-Z$  and  $\beta + \gamma$  by  $-(\beta + \gamma)$ .

Equations 2-9 and 2-10 reveal that the model of equation 2-2 is rate - independent, i.e. independent of the value of velocity. Rather, only the sign of velocity determines the ascending and descending branches. Furthermore, equation 2-12 restricts the values of constants  $A$ ,  $\beta$  and  $\gamma$  to  $A = \beta + \gamma$  so that  $Z_{\max} = 1$ . Explicit expressions for  $Z$  are possible only for  $n=1$  or 2:

$$Z = \frac{A}{\beta + \gamma} \left\{ 1 - \exp \left[ -(\beta + \gamma) \frac{U}{Y} \right] \right\} + C, \quad \text{for } n=1 \quad (2-13)$$

$$Z = \left( \frac{A}{\beta + \gamma} \right)^{\frac{1}{2}} \tanh \left[ (\beta + \gamma)^2 \frac{U}{Y} \right] + C, \quad \text{for } n=2 \quad (2-14)$$

For  $A = \beta + \gamma$  as required for  $Z_{\max} = 1$ , equations 2-13 and 2-14 show that  $Z$  represents a smooth approximation to the unit step function. Increasing values of  $n$  result in approximations that are closer to the step function with the case  $n \rightarrow \infty$  presumably reproducing the step function itself. Interestingly, the actual values of constants  $\beta$  and  $\gamma$  do not play any role. Rather, only their sum plays a role.

Based on the conclusions of this analytical solution and comparisons of experimental and analytical compression - tension loops, the following values were selected :  $A=3.0$ ,



$\beta=0.0$ ,  $\gamma=3.0$  ( $\lambda = \beta + \gamma$ ) and  $n=1$ . Values of displacement quantity  $Y$  were different for each isolator as shown in Table 2-IV. Comparisons of experimental and analytical force - displacement loops of the four isolators in compression - tension mode are presented in Figures 2-12 to 2-15. Each of these loops is for a specific initial compression force imposed to the isolator prior to initiation of the cyclic motion and for five cycles of motion. The loops for the stiff isolator No.4 are for small amplitudes of displacement. Evidently the analytical model predicts the experimental behavior with good accuracy.

Table 2-I - Geometrical Characteristics of Tested Wire Rope Isolators (1 in.= 25.4 mm)

DESIGNATION	TYPE	TESTING DIRECTION	NUMBER OF COILS	DIAMETER OF ROPE (inch)	L (inch)	W (inch)	H (inch)
ISOLATOR 1	ARCH	COMPR/ROLL	2	0.500	11.25	4.60	4.75
ISOLATOR 2	HELICAL	"	8	0.500	7.00	5.60	4.90
ISOLATOR 3	ARCH	"	4	0.500	11.25	4.60	4.75
ISOLATOR 4	HELICAL	"	8	0.625	10.50	6.00	4.70
ISOLATOR 5	HELICAL	SHEAR	8	0.375	8.50	4.13	3.00

Table 2-II - Parameters of Model of Isolators in Roll and Shear Directions

(1 in. = 25.4 mm, 1 Kip = 4.46 kN)

	DIRECTION	$K_x$ (Kip/in)	$Y$ (inch)	$Q$ (Kip)	$F_y$ (Kip)	$\alpha$
ISOLATOR 1	ROLL	0.172	0.010	0.013	0.0147	0.1169
ISOLATOR 2	ROLL	0.171	0.010	0.028	0.0294	0.0581
ISOLATOR 3	ROLL	0.365	0.015	0.030	0.0355	0.1543
ISOLATOR 4	ROLL	0.684	0.015	0.100	0.1103	0.0931
ISOLATOR 5	SHEAR	0.240	0.010	0.014	0.0164	0.1463

Table 2-III - Coefficients in Function  $F_0$  of Model of Wire Rope Isolators in Vertical Direction (1 in. = 25.4 mm, 1 Kip = 4.46 kN)

	$Q_1$ (Kip)	$A_0$	N	$a_1$ (in <sup>-1</sup> )	$a_2$ (in <sup>-2</sup> )	$a_3$ (in <sup>-3</sup> )
ISOLATOR 1	-0.290	1.00	3	1.7860	0.3510	0.202
ISOLATOR 2	-0.790	1.04	3	0.8523	-0.0367	0.151
ISOLATOR 3	-0.470	1.00	1	2.0797	-	-
ISOLATOR 4	-0.905	1.00	3	1.3120	-0.5730	0.336

Table 2-IV - Coefficients of Function  $F_D$  of Model of Wire Rope Isolators in Vertical Direction (1 in. = 25.4 mm, 1 Kip = 4.46 kN)

	Coefficients of Function $F_D$						Y (in)
	$Q_2$ (Kip)	M	$b_0$	$b_1$ (in <sup>-1</sup> )	$b_2$ (in <sup>-2</sup> )	$b_3$ (in <sup>-3</sup> )	
ISOLATOR 1	0.001	3	3.555	1.5734	1.132	0.252	0.100
ISOLATOR 2	0.001	1	4.701	0.6496	-	-	0.100
ISOLATOR 3	0.001	1	4.090	0.8960	-	-	0.100
ISOLATOR 4	0.001	1	5.882	1.2300	-	-	0.055

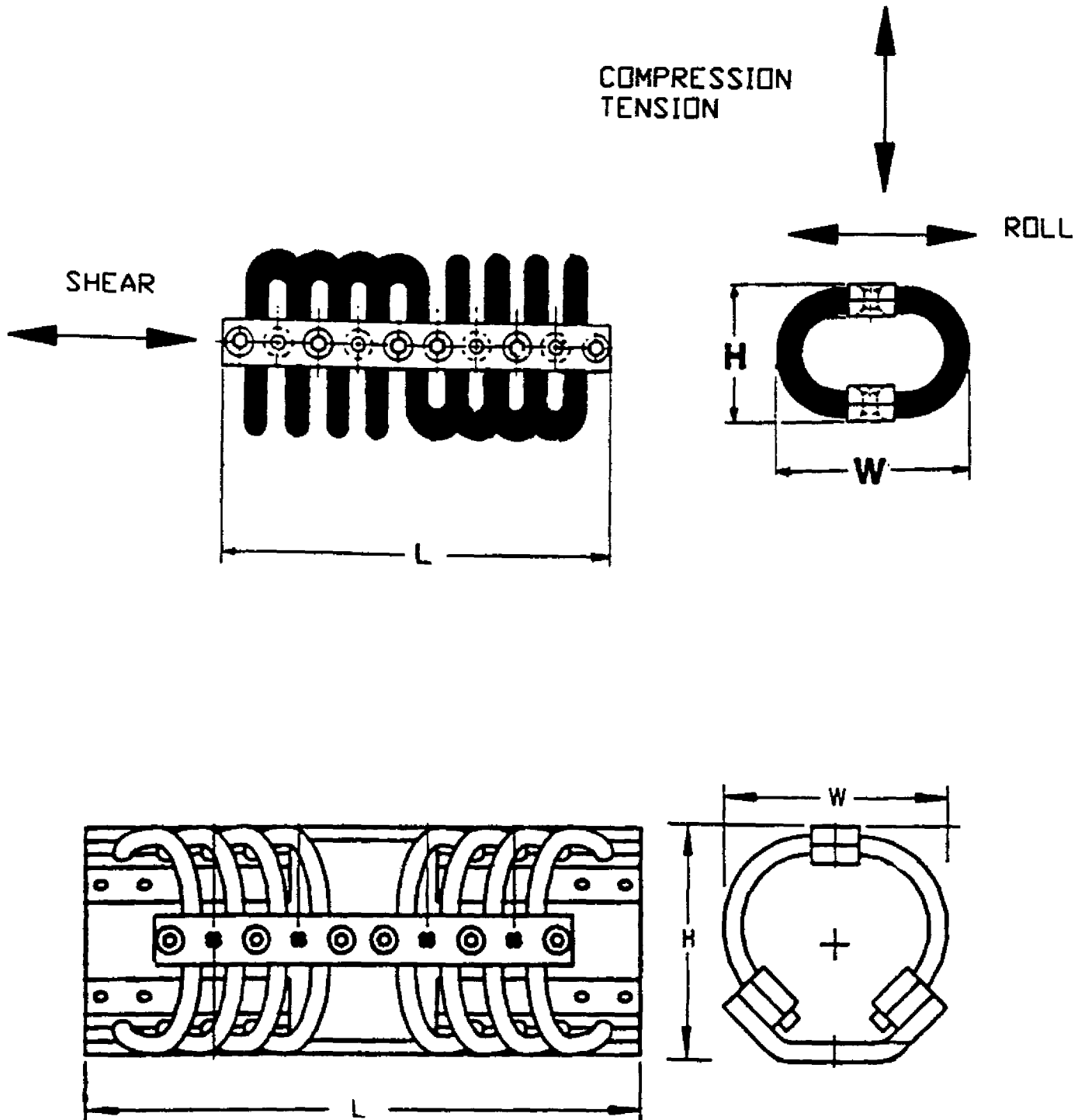


Figure 2-1 Geometrical Characteristics of Helical and Arch Wire Rope Isolators.

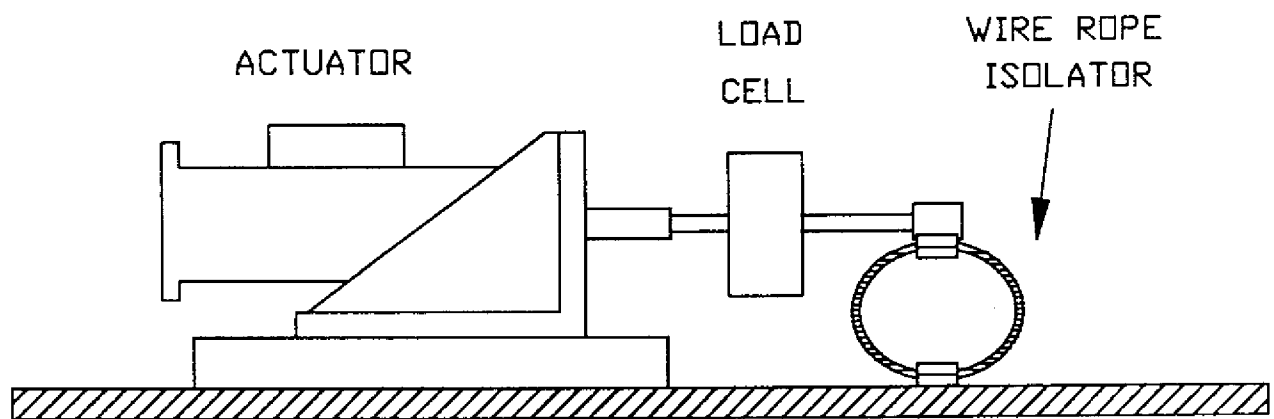


Figure 2-2 Arrangement for Testing Wire Rope Isolators (No.1 to 4) in Roll Direction.

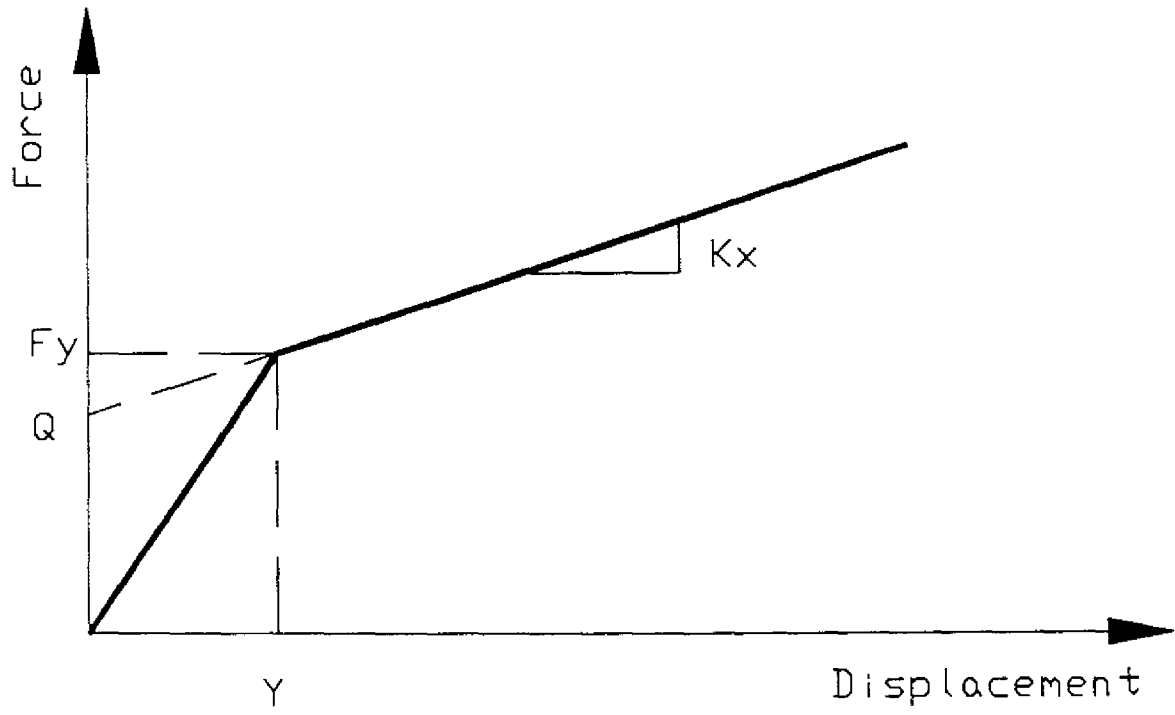


Figure 2-3 Parameters in Bilinear Model.

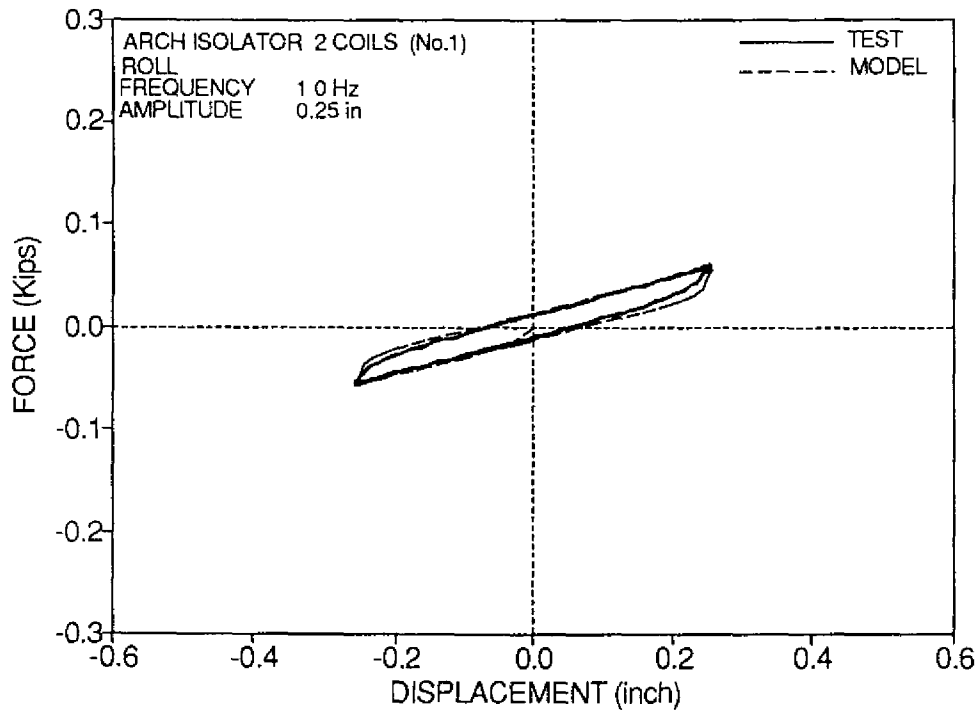
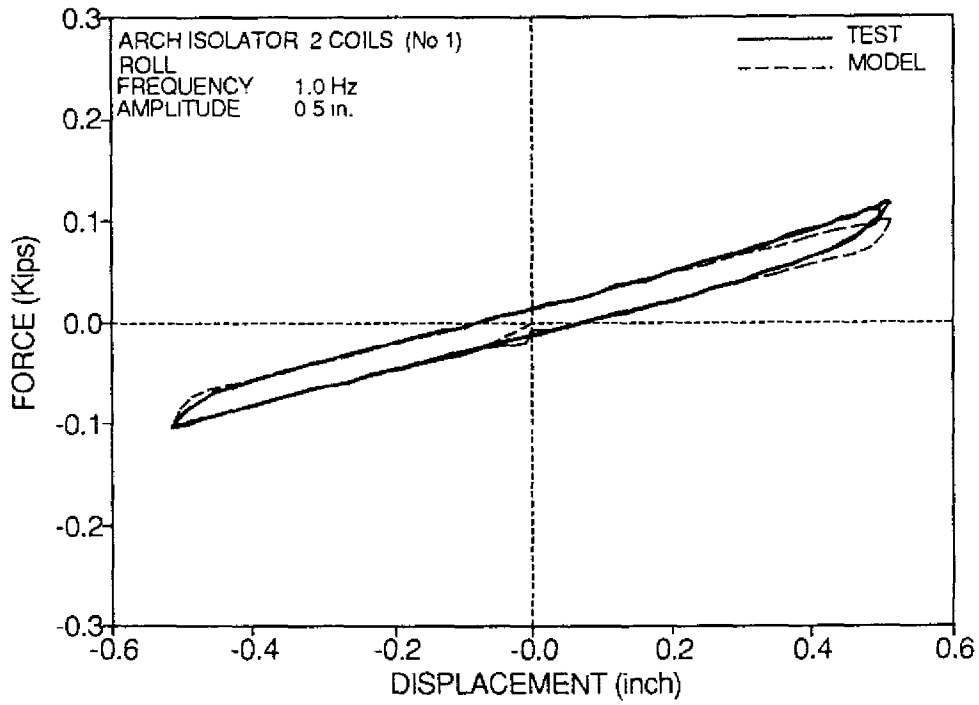


Figure 2-4 Comparison of Experimental and Analytical Force - Displacement Loops of Isolator No.1 subjected to Roll Motion (1 in.= 25.4 mm, 1 Kip= 4.46 kN).



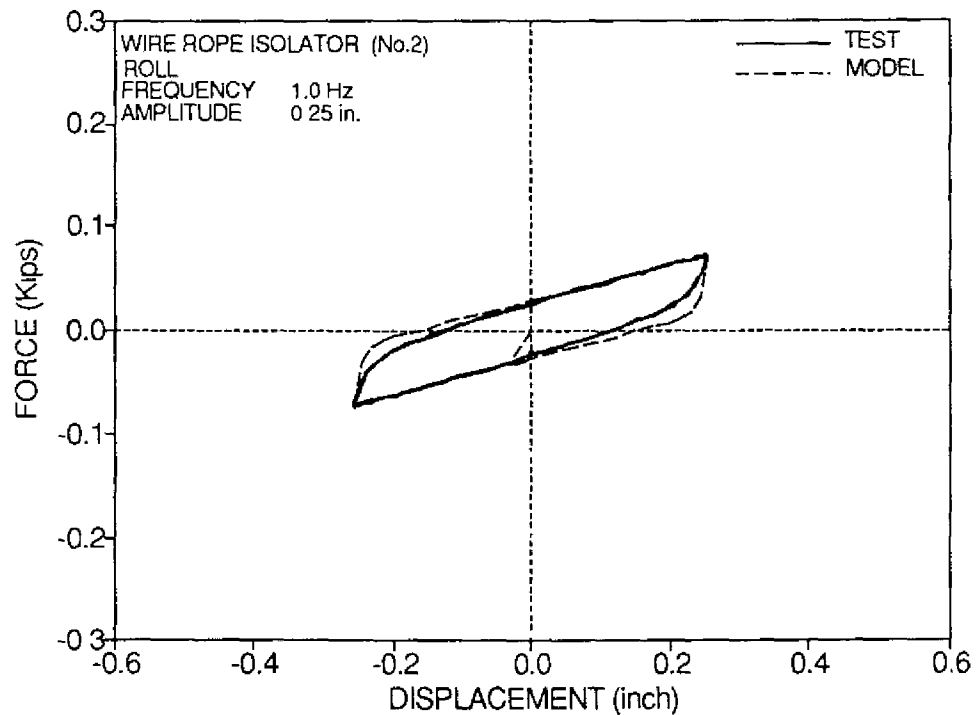
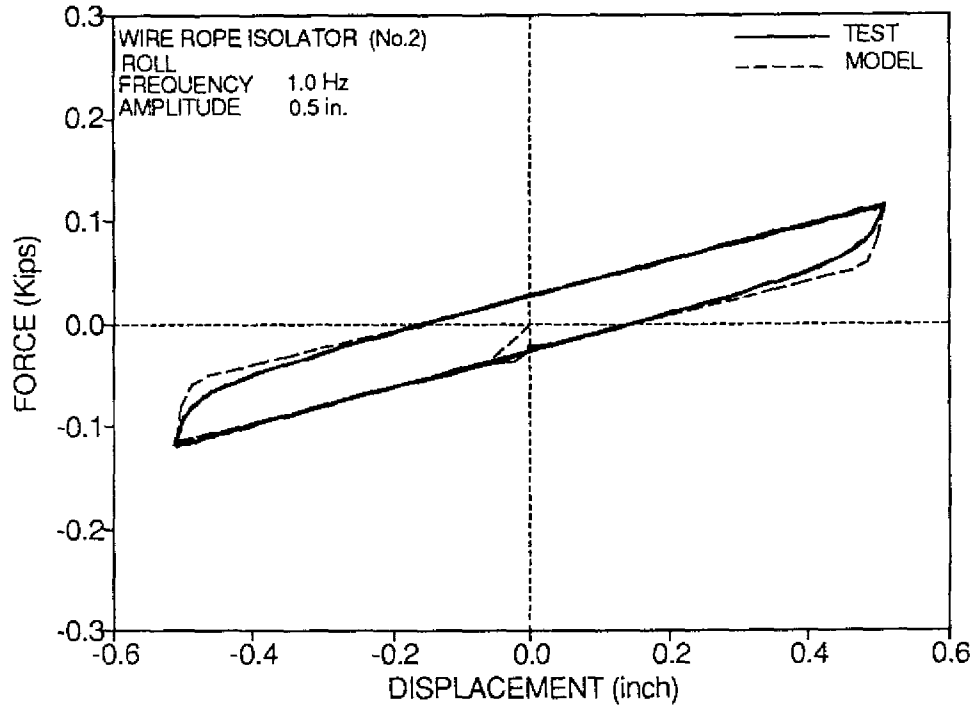


Figure 2-5 Comparison of Experimental and Analytical Force - Displacement Loops of Isolator No.2 subjected to Roll Motion (1 in.= 25.4 mm, 1 Kip= 4.46 kN).

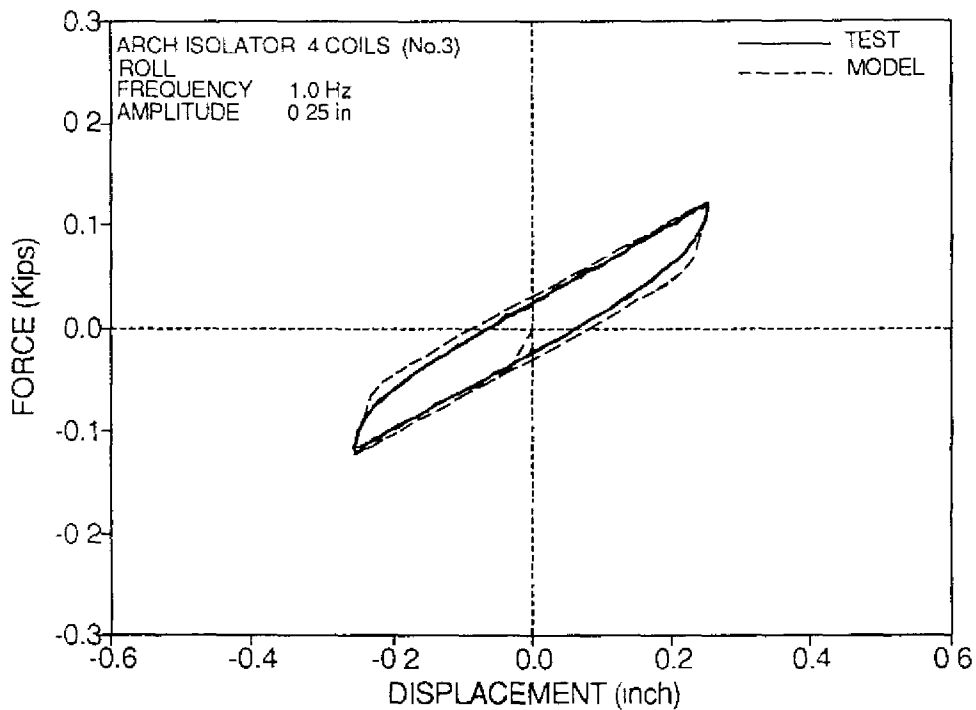
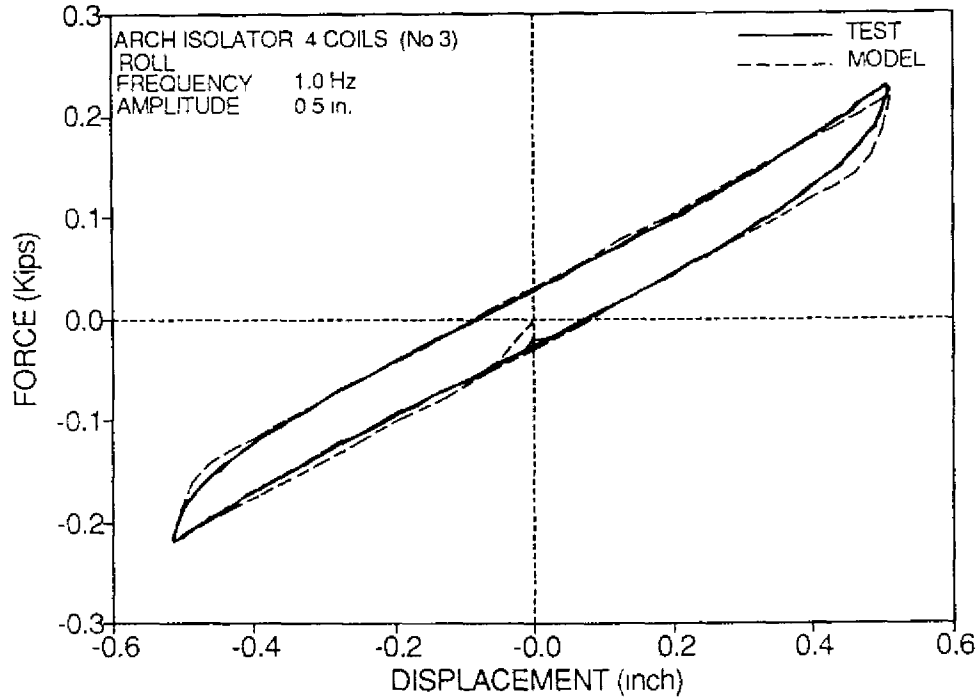


Figure 2-6 Comparison of Experimental and Analytical Force - Displacement Loops of Isolator No.3 subjected to Roll Motion (1 in.= 25.4 mm, 1 Kip= 4.46 kN).

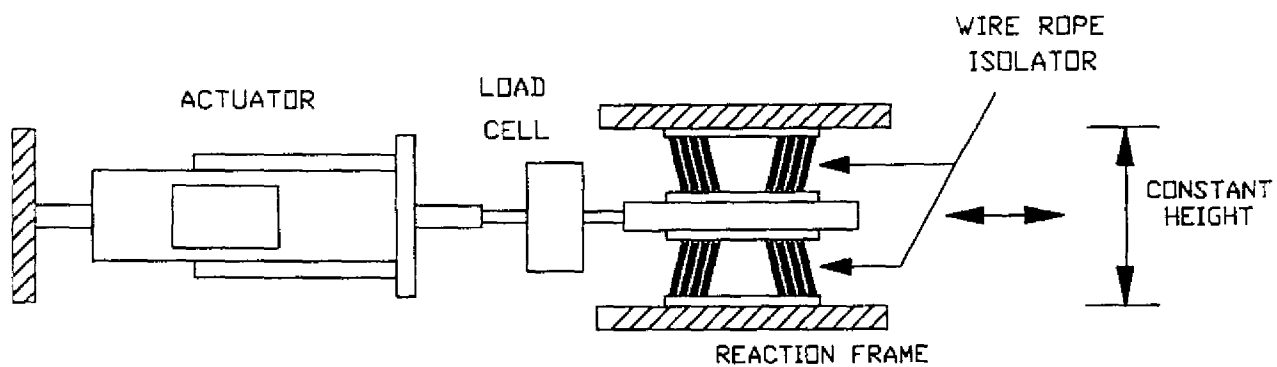


Figure 2-7 Arrangement for Testing Wire Rope Isolators (No.5) while Maintaining Constant Height.

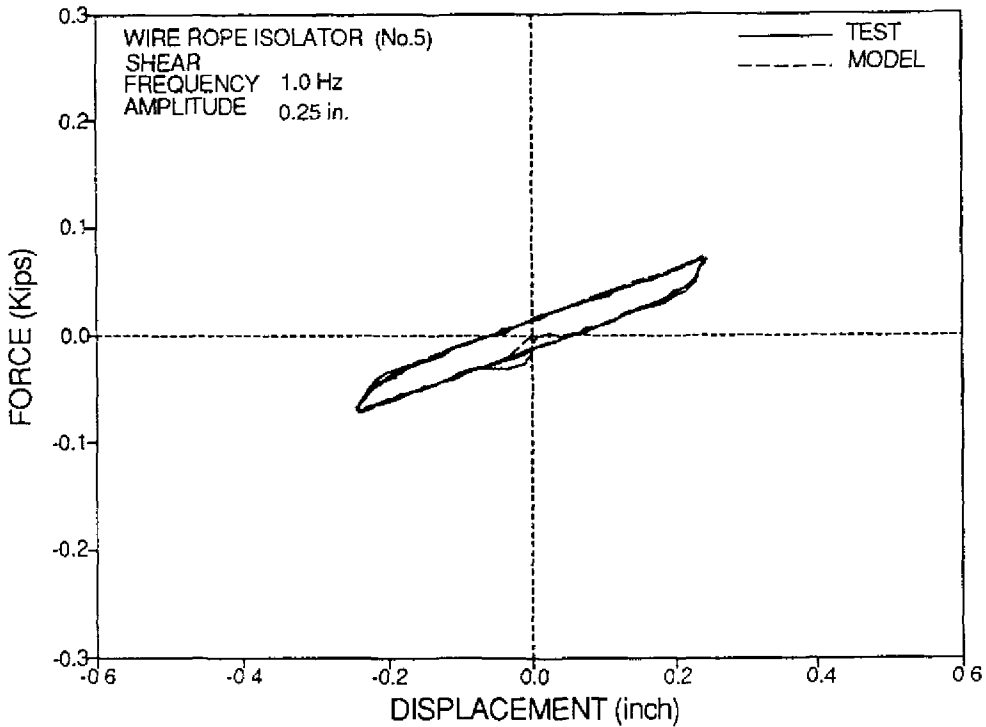
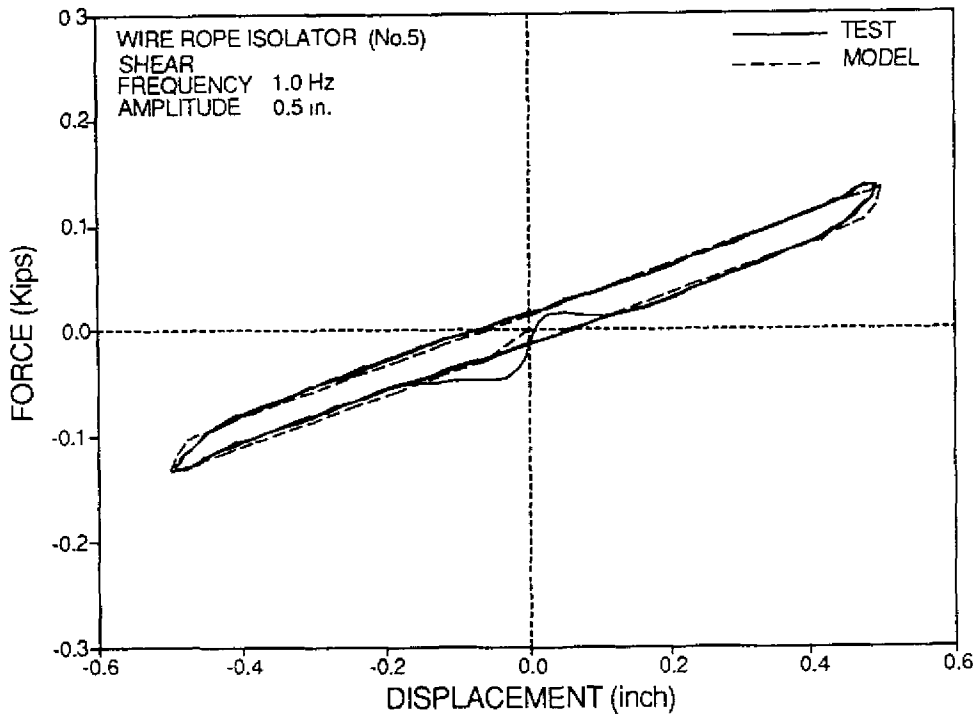


Figure 2-8 Comparison of Experimental and Analytical Force - Displacement Loops of Isolator No.5 subjected to Shear Motion (1 in.= 25.4 mm, 1 Kip= 4.46 kN).

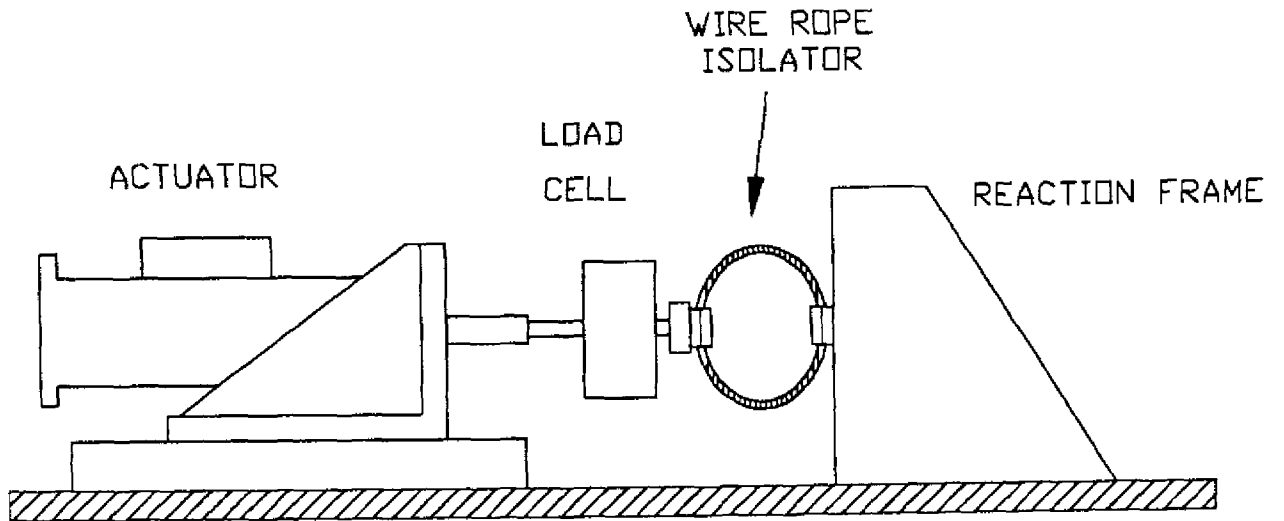


Figure 2-9 Arrangement for Testing Wire Rope Isolators in Compression - Tension.

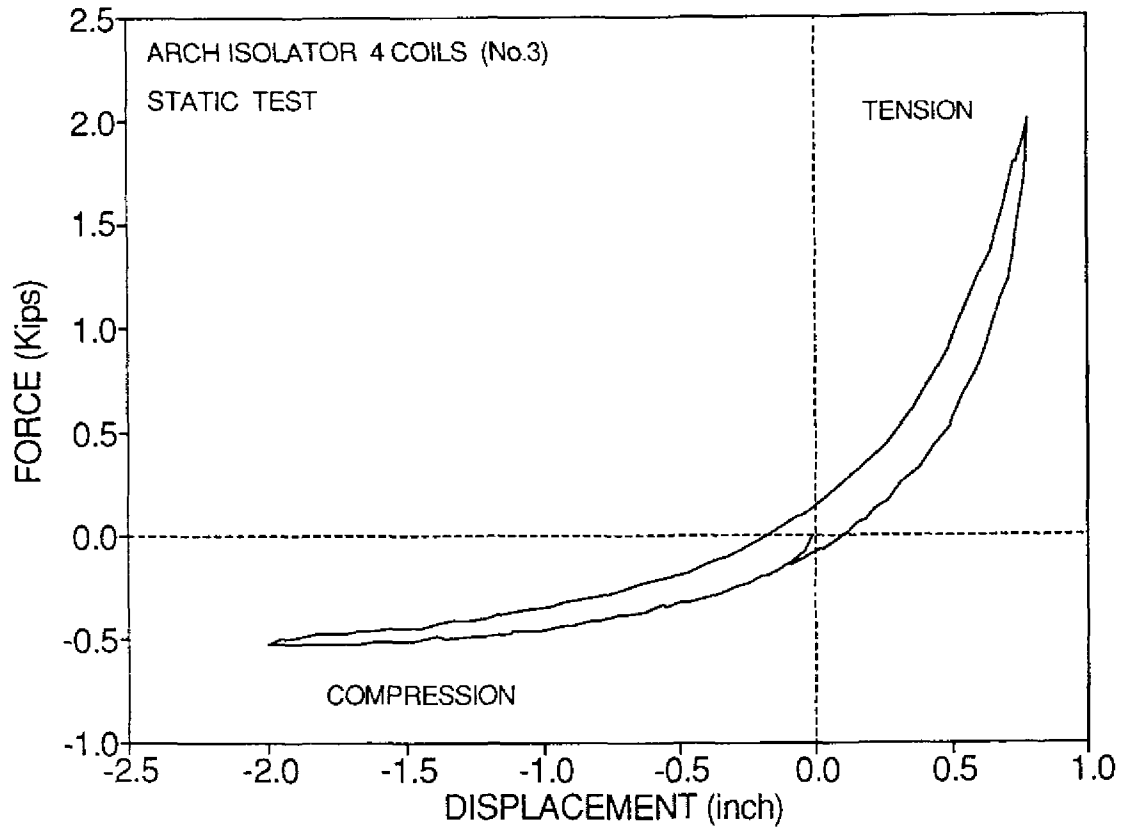


Figure 2-10 Typical Force - Displacement Loop of Wire Rope Isolators in Compression - Tension (1 in. = 25.4 mm, 1 Kip = 4.46 kN).

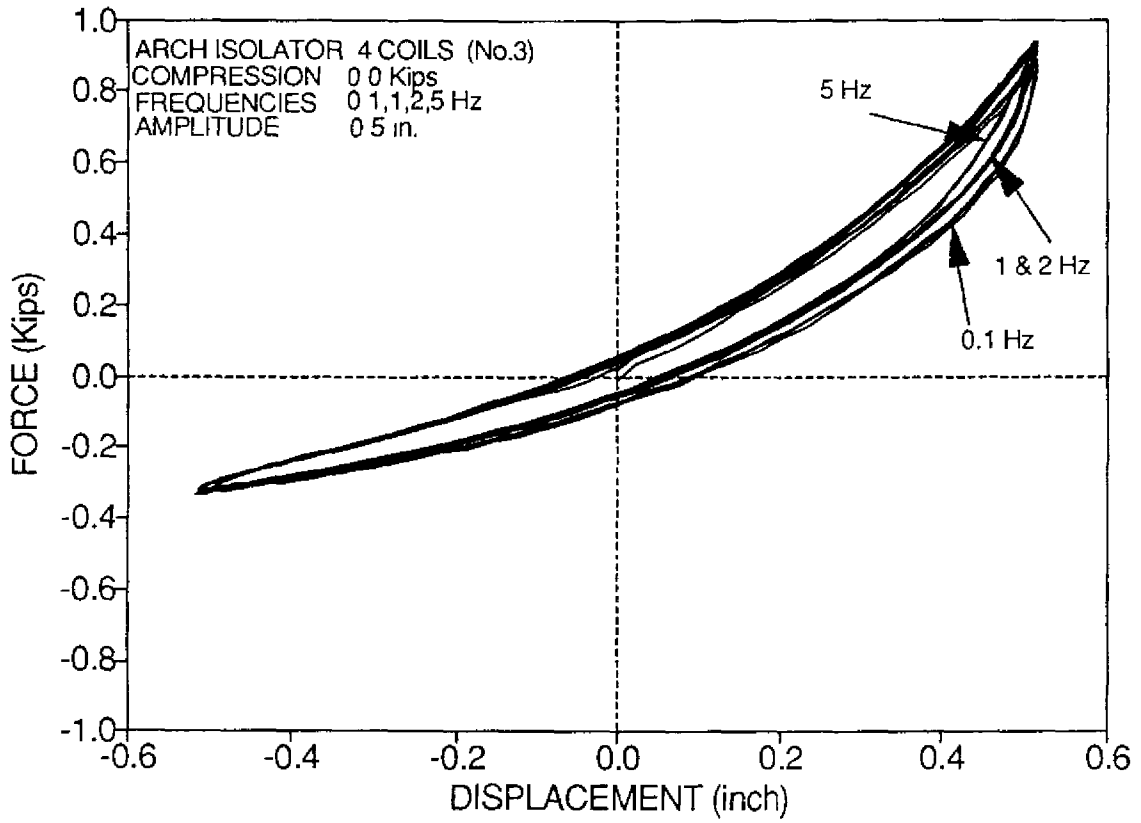


Figure 2-11 Force - Displacement Loops in Compression - Tension for Cyclic Motion (1 in.= 25.4 mm, 1 Kip= 4.46 kN).

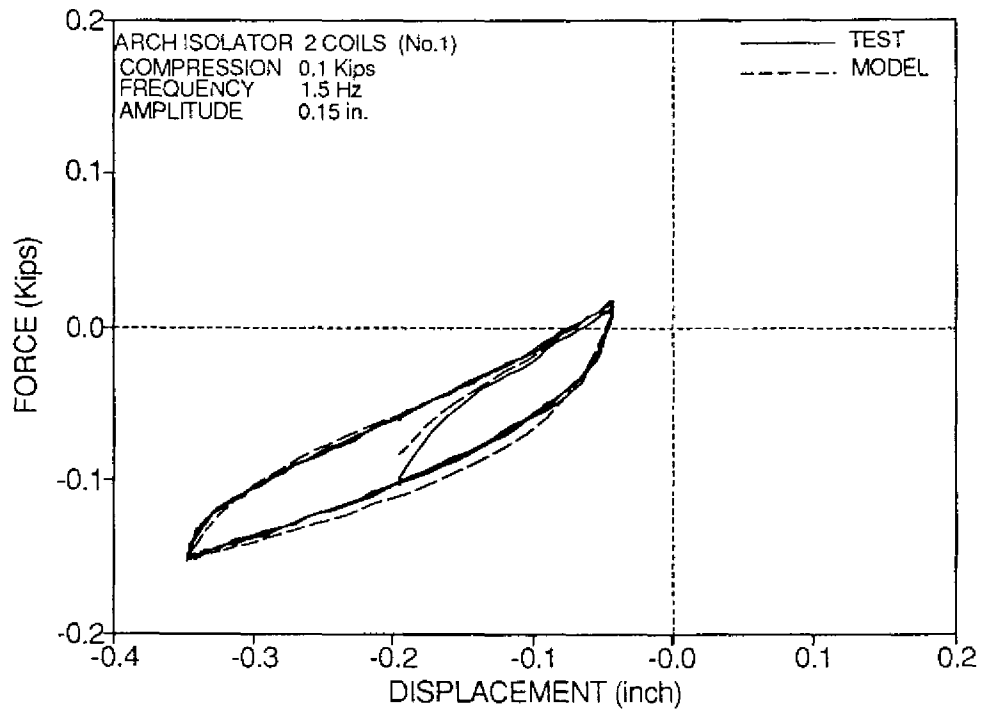
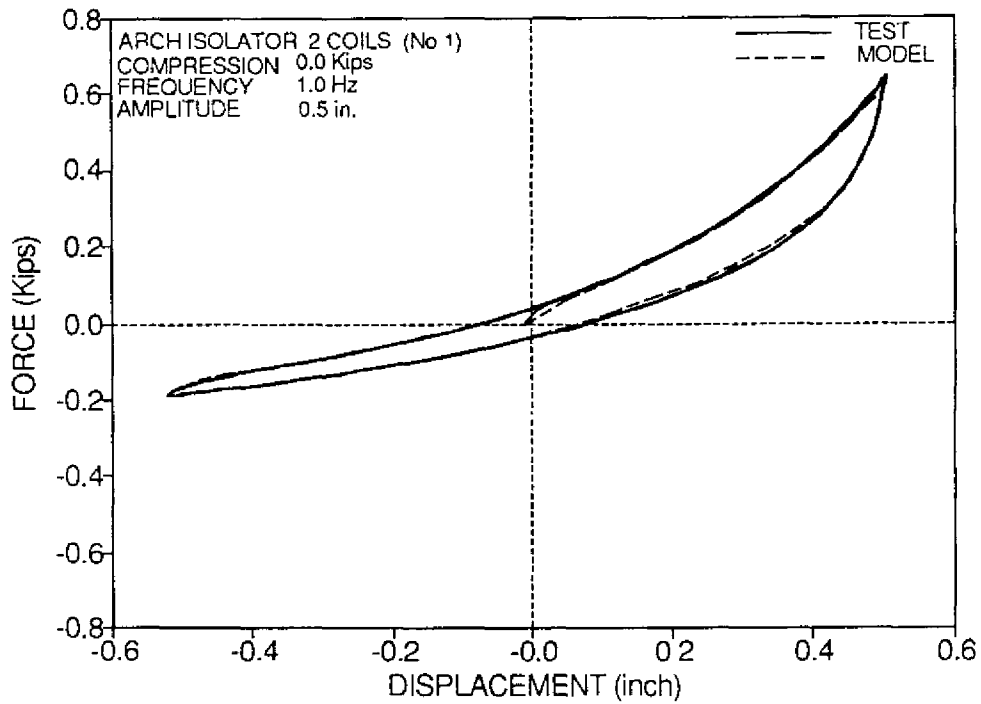


Figure 2-12 Comparison of Experimental and Analytical Force - Displacement Loops of Isolator No.1 subjected to Compression-Tension ( 1 in.= 25.4 mm, 1 Kip= 4.46 kN) .



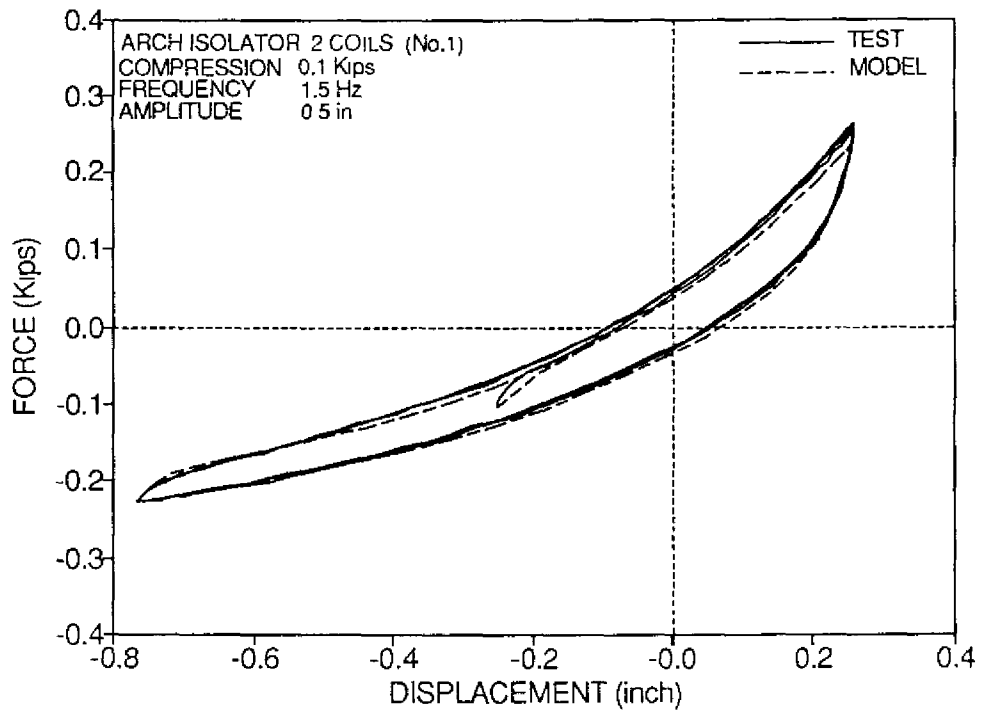
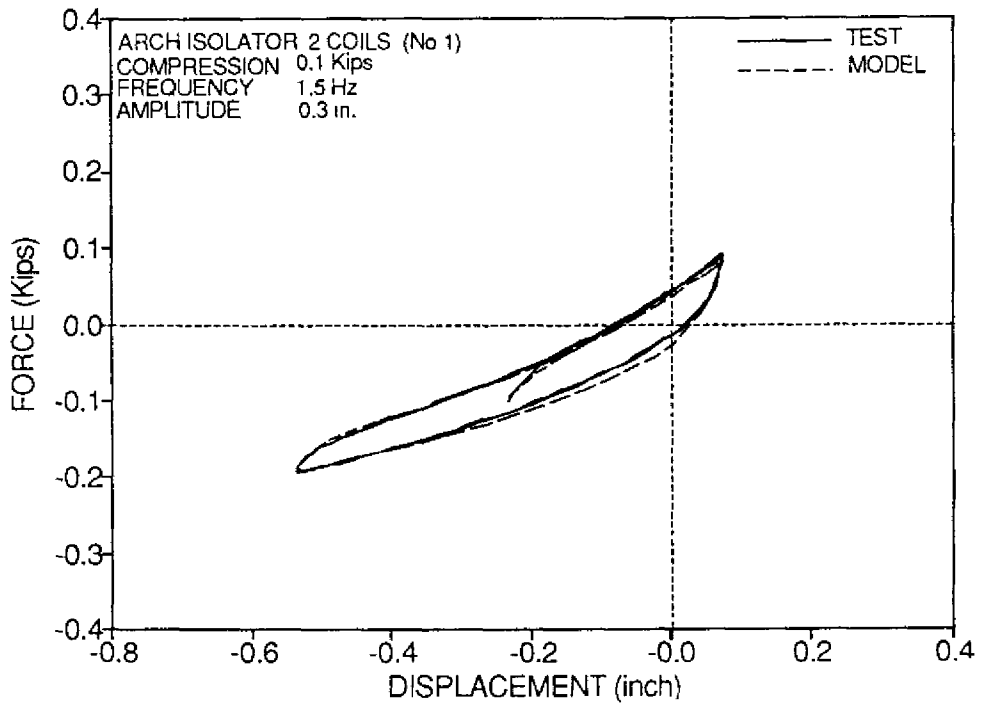


Figure 2-12 Continued.

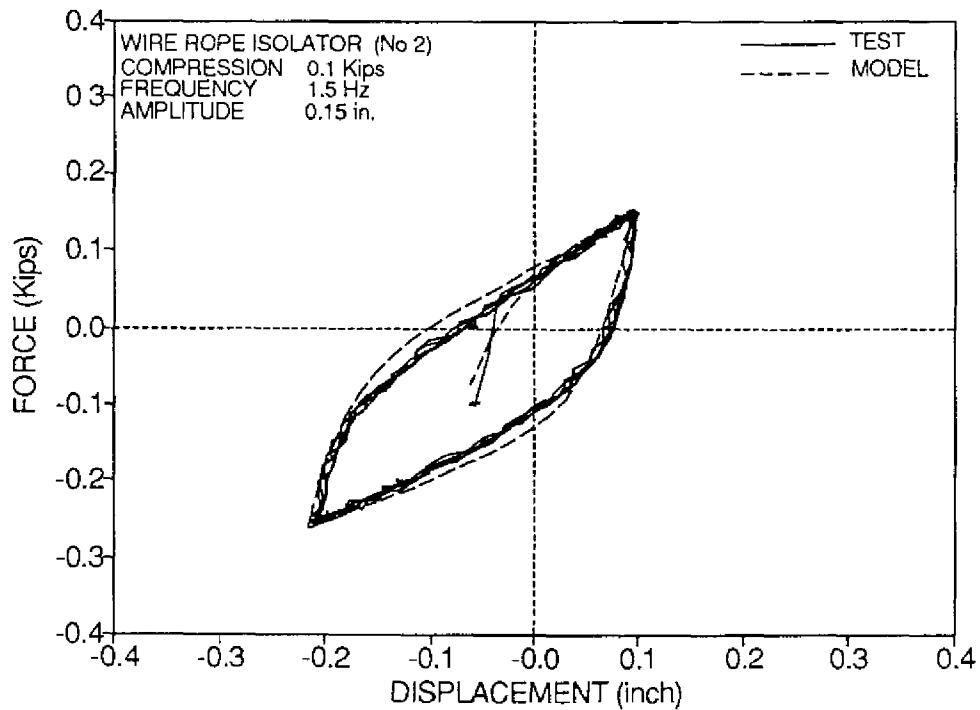
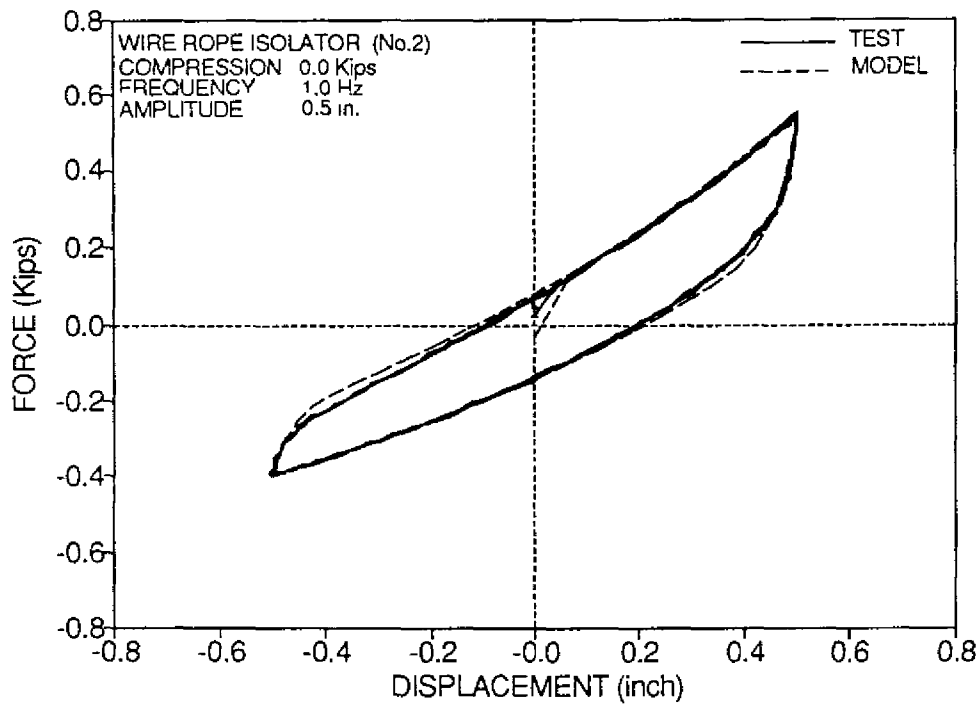


Figure 2-13 Comparison of Experimental and Analytical Force - Displacement Loops of Isolator No.2 subjected to Compression-Tension ( 1 in.= 25.4 mm, 1 Kip= 4.46 kN).

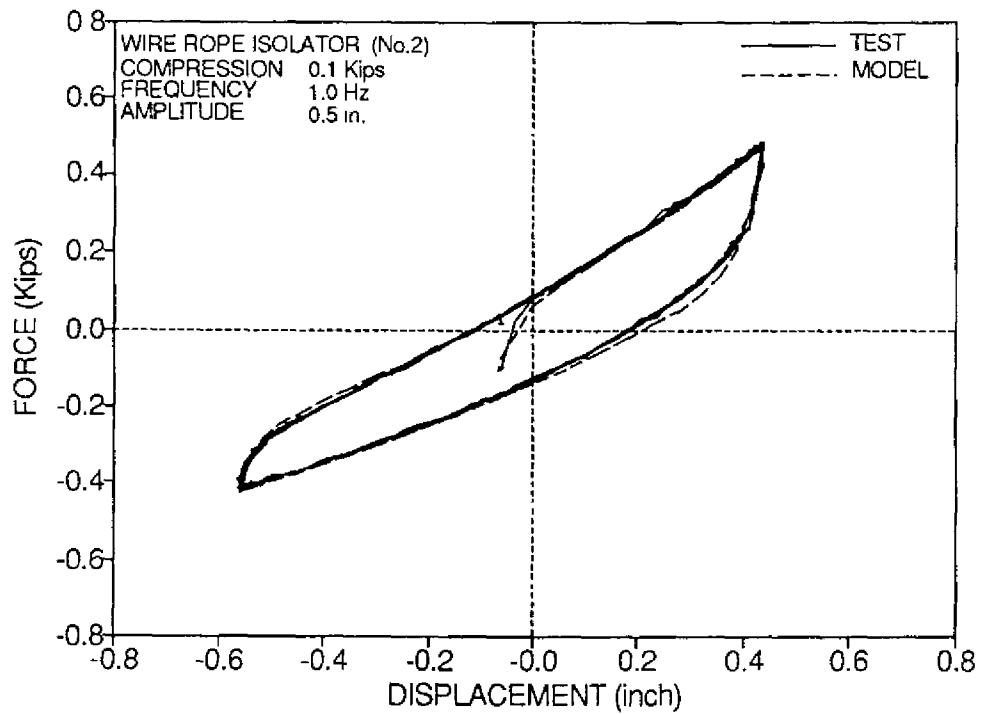
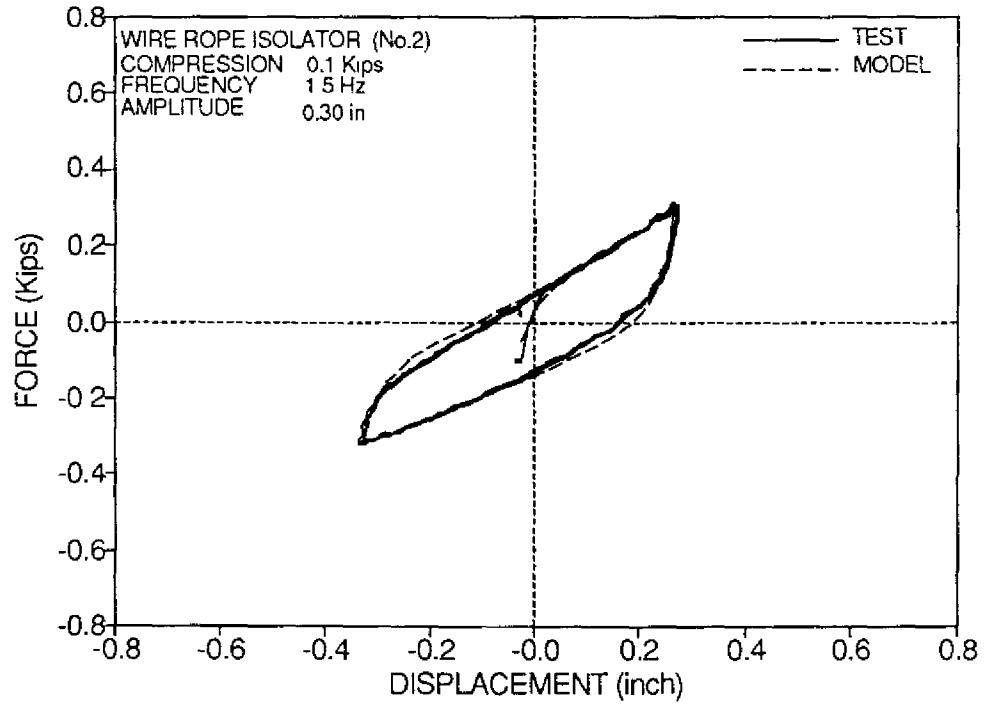


Figure 2-13 Continued.

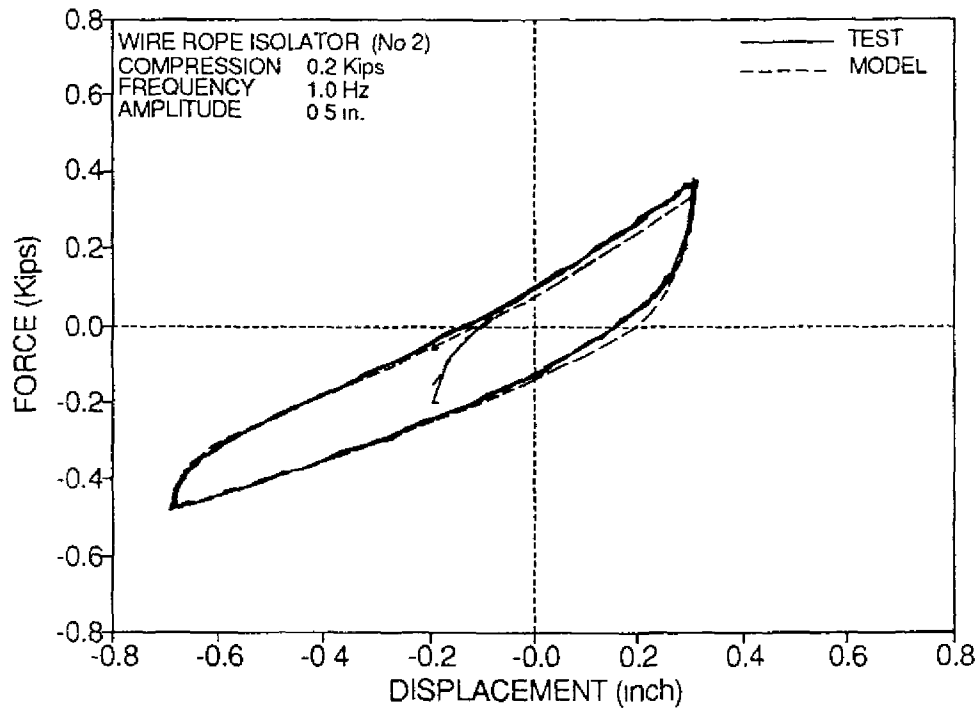
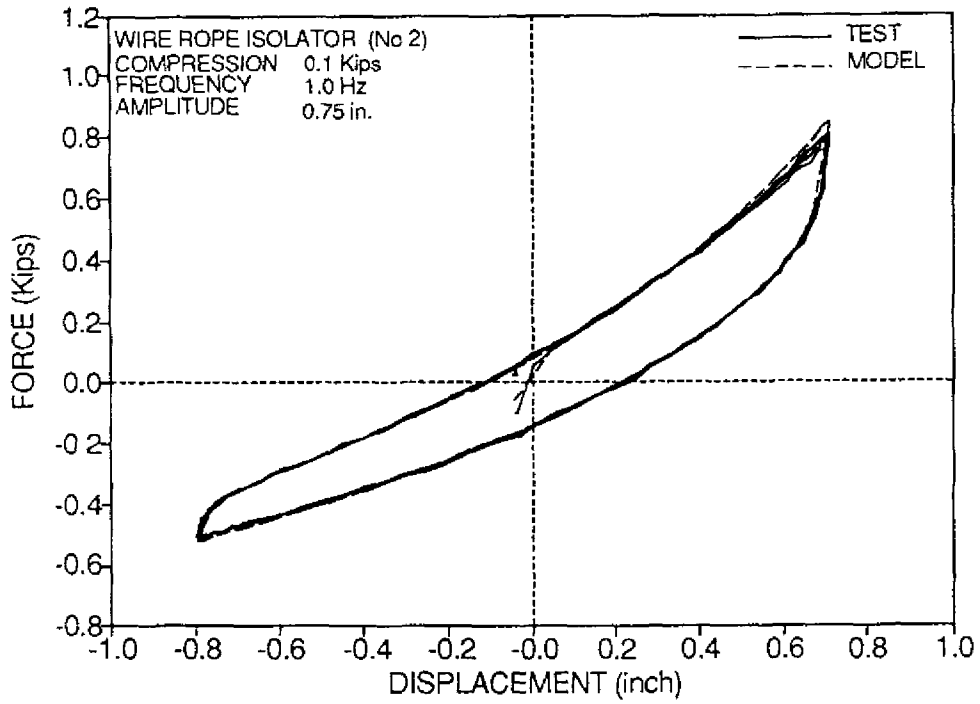


Figure 2-13 Continued.

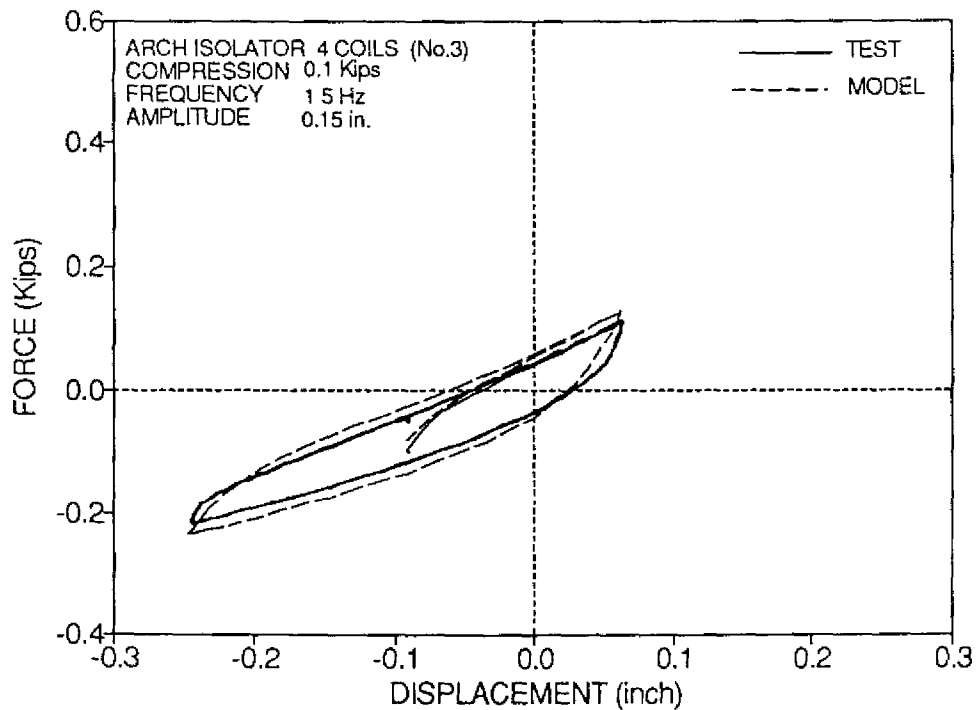
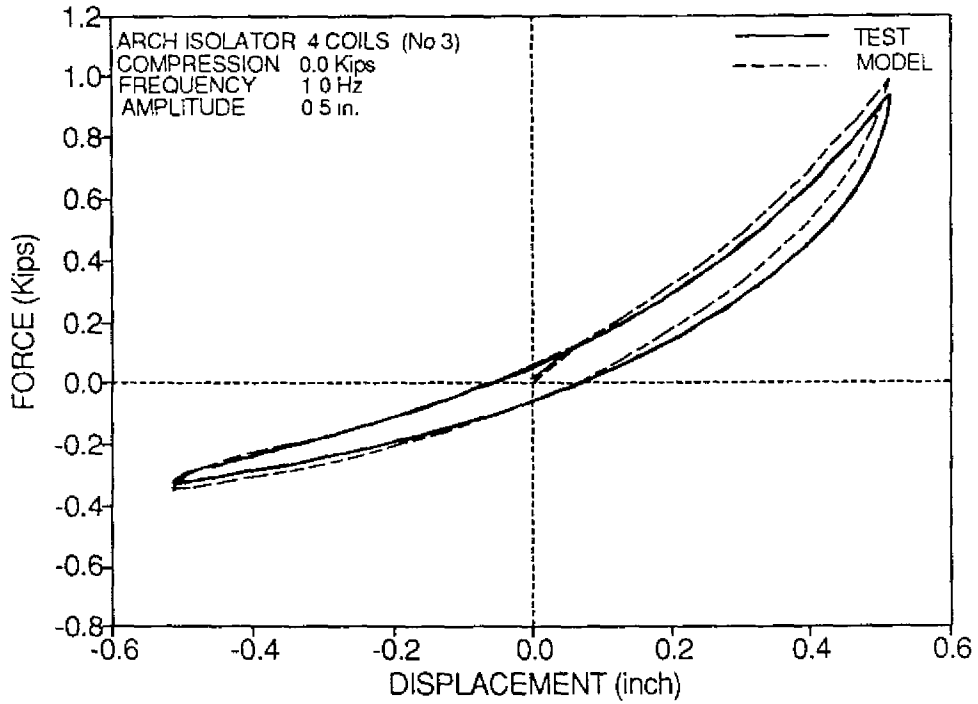


Figure 2-14 Comparison of Experimental and Analytical Force - Displacement Loops of Isolator No.3 subjected to Compression-Tension ( 1 in.= 25.4 mm, 1 Kip= 4.46 kN) .

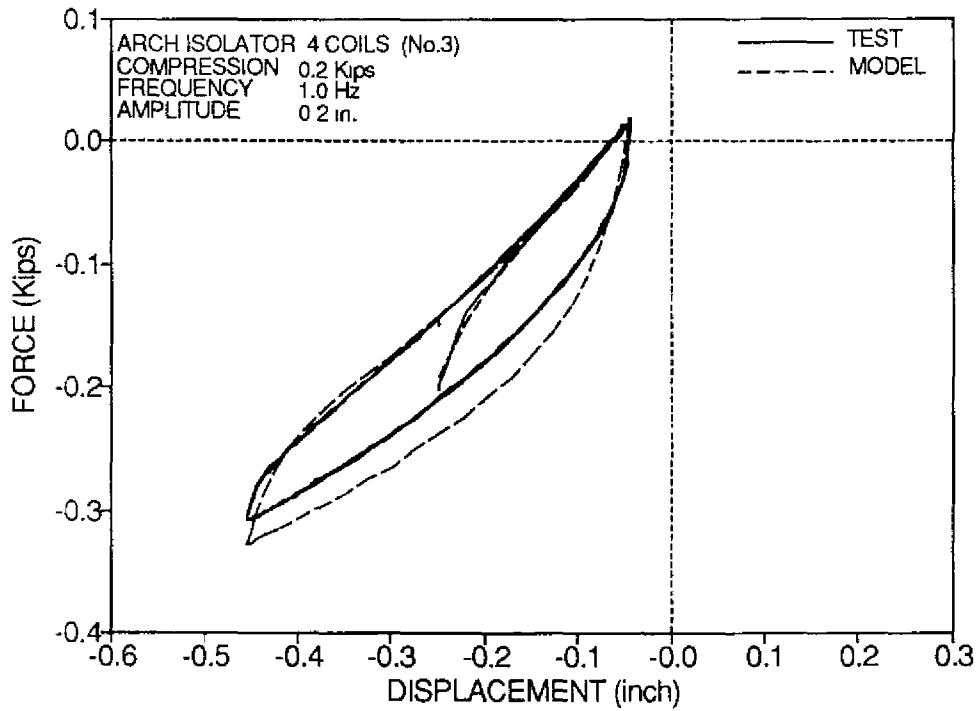
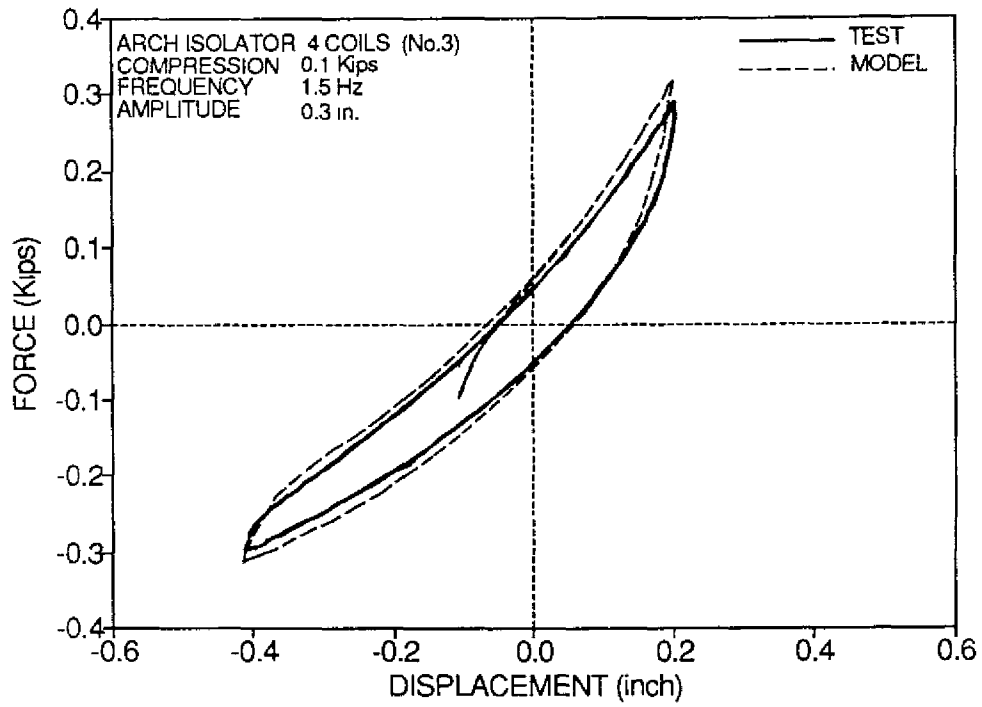


Figure 2-14 Continued.

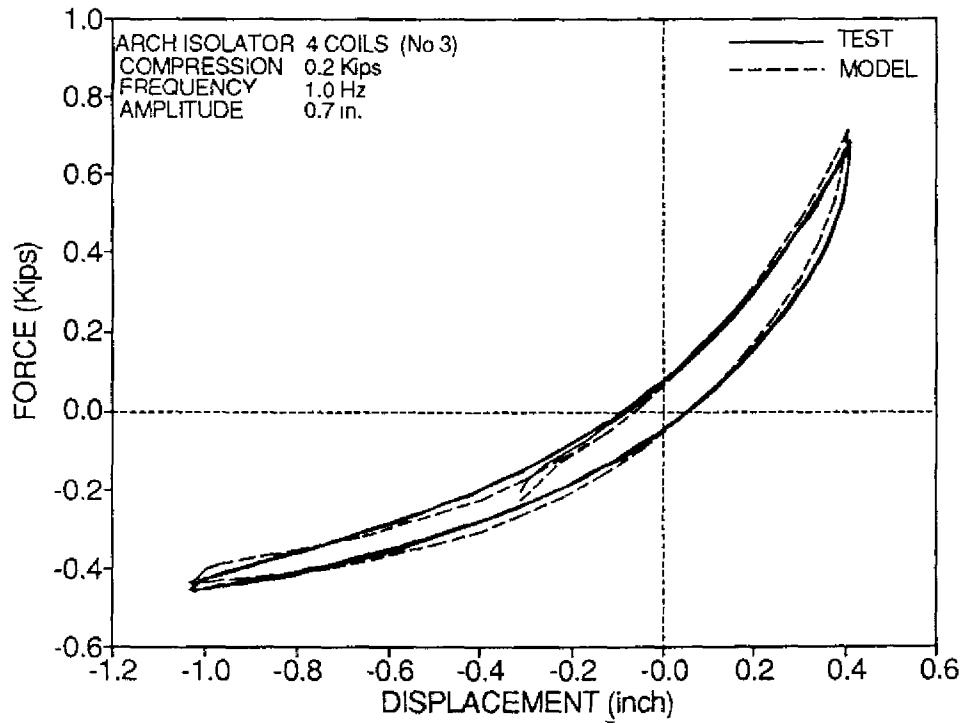
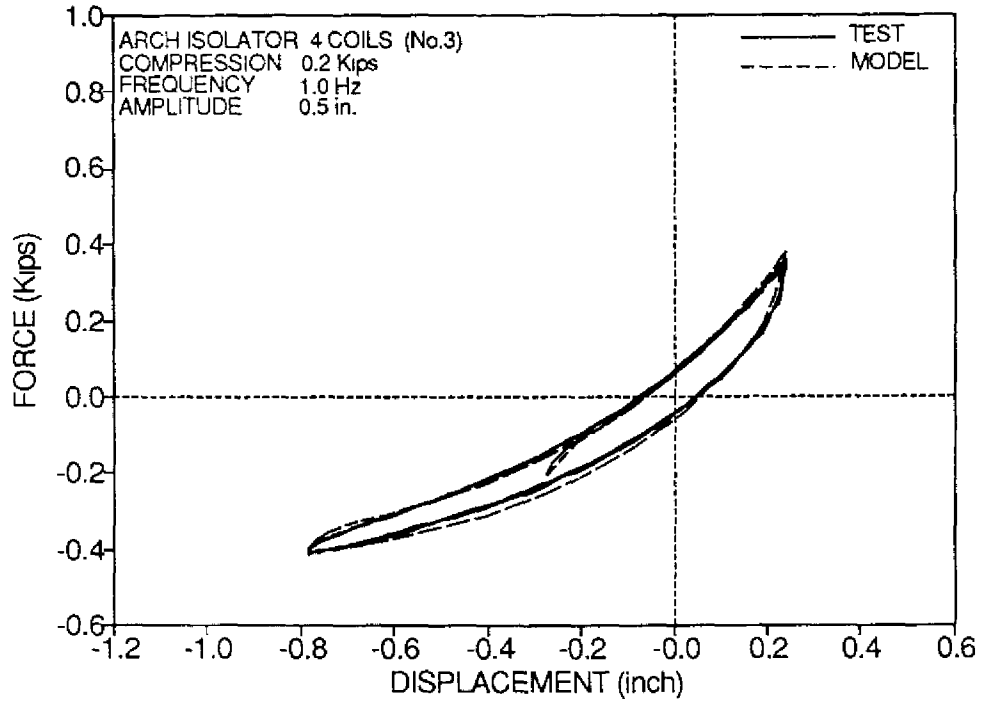


Figure 2-14 Continued.

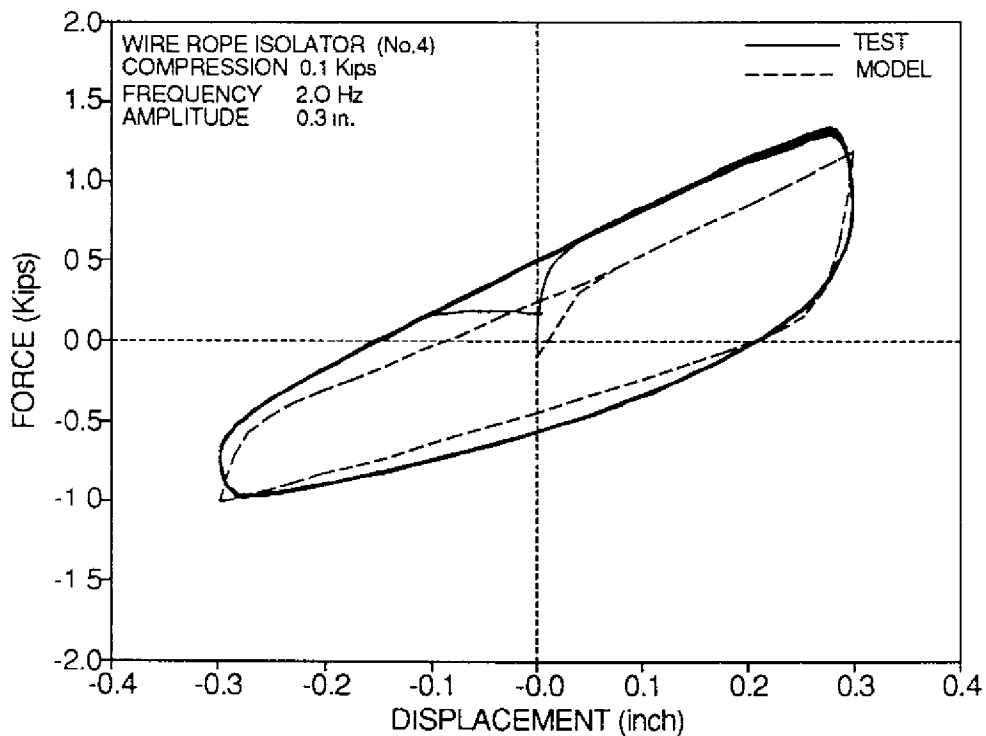
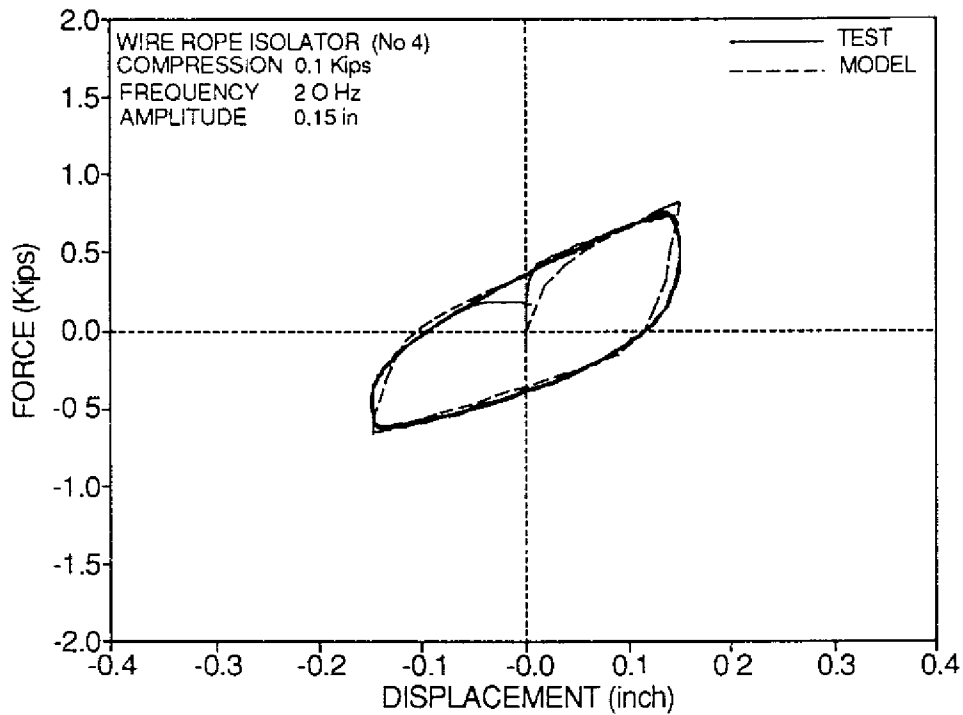


Figure 2-15 Comparison of Experimental and Analytical Force - Displacement Loops of Isolator No.4 subjected to Compression-Tension ( 1 in.= 25.4 mm, 1 Kip= 4.46 kN) .